Supporting Information

Allylic oxidation of olefins with a manganese-based metal-organic framework

Jingwen Chen,[a,b] Minda Chen,[b] Biying Zhang,[b] Renfeng Nie,[b,c] Ao Huang,[b] Tian Wei Goh,[b,d] Alexander Volkov,[b] Zhiguo Zhang,*[a] Qilong Ren[a] and Wenyu Huang*[b,d]

[a] Key Laboratory of Biomass Chemical Engineering of Ministry of Education, College of Chemical and Biological Engineering, Zhejiang University, Zheda Road 38, Hangzhou 310027, P. R. China

[b] Department of Chemistry, Iowa State University, Ames, IA 50011, USA

[c] School of Chemistry and Chemical Engineering, Hubei University, Wuhan 430062, PR China

[d] Ames Laboratory, US Department of Energy, Ames, IA 50011, USA

E-mail: zhiguo.zhang@zju.edu.cn, whuang@iastate.edu

1. Materials and Methods

All chemicals and solvents were obtained from commercial sources and were used as received without further purification unless otherwise stated.

CPF-5 was degassed at 373 K for 24 h before measuring the BET surface area on a Quantachrome AUTOSORB-IQ2-MP instrument at 77 K. The powder X-ray diffraction (XRD) patterns were obtained on STOE Stadi P powder diffractometer using Cu Kα radiation (40 kV, 40 mA, $\lambda = 0.1541$ nm). ^{1}H NMR and ^{13}C NMR spectra were measured on a Varian MR-400 device with a frequency of 400 MHz. The product was analyzed using gas chromatograph equipped with a flame ionization detector and Agilent 6890N/5975 gas chromatography-mass spectroscopy (GC-MS) equipped with an HP-5MS capillary column (30 m × 0.25 mm × 0.25 μm). The X-ray photoelectron spectroscopy (XPS) measurements were performed using a Kratos Amicus/ESCA 3400 instrument. The sample was irradiated with 240 W unmonochromated Mg *Kα* X-rays, and photoelectrons emitted at 0° from the surface normal were energy analyzed using a DuPont type analyzer. All spectra were energy calibrated with measured C 1*s* peak position at 284.6 eV. Inductively coupled plasma optical emission spectroscopy (ICP-OES) analysis was performed on Varian ICP 730-OES to determine the actual amount of Mn. The samples were calcinated at 550 °C for 5 h and digested in boiling aqua regia until all solid dissolved completely.

2. Preparation of CPF-5

2.1 Synthesis of ligand

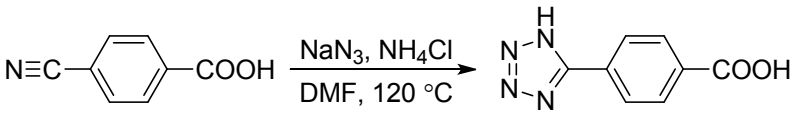

4-Tetrazole benzoic acid was synthesized via a method modified from literature [1]. Ammonium chloride (5.89 g, 0.11 mol), sodium azide (7.16 g, 0.11 mmol) and DMF (100 mL) mixed and stirred at r.t. for 30 min. 4-Cyanobenzoic acid (13.7 g, 0.093 mmol) was added to the above solution and heated to 120 °C, the temperature was kept at 120 °C under reflux for 24 h. After cooling to r.t., 1 M HCl solution (~186 mL) was added (pH ~2 as indicated by pH paper). The white solid was collected by filtration and washed with water thoroughly. The solid was dried and recrystallized from ethanol. The white crystal was dried under vacuum at 60 °C to remove the residual solvent (Yield: 82%).

4-Tetrazole benzoic acid: ^{1}H NMR (400 MHz, DMSO-d_6): 13.33 (brs, 1H), 8.15 (d, 4H), 3.86 (brs, 1H) ppm. ^{13}C NMR (100 MHz, DMSO-d_6): 166.63, 132.96, 130.30, 127.17 ppm. MS (EI$^+$) m/z: calcd. for $C_8H_7N_4O_2$: 191.06 [M+H$^+$]; found: 191.20. ATR FTIR (cm^{-1}): 3226, 3094, 2552, 1807, 1678, 1568, 1438, 1317, 1284, 1087, 817.

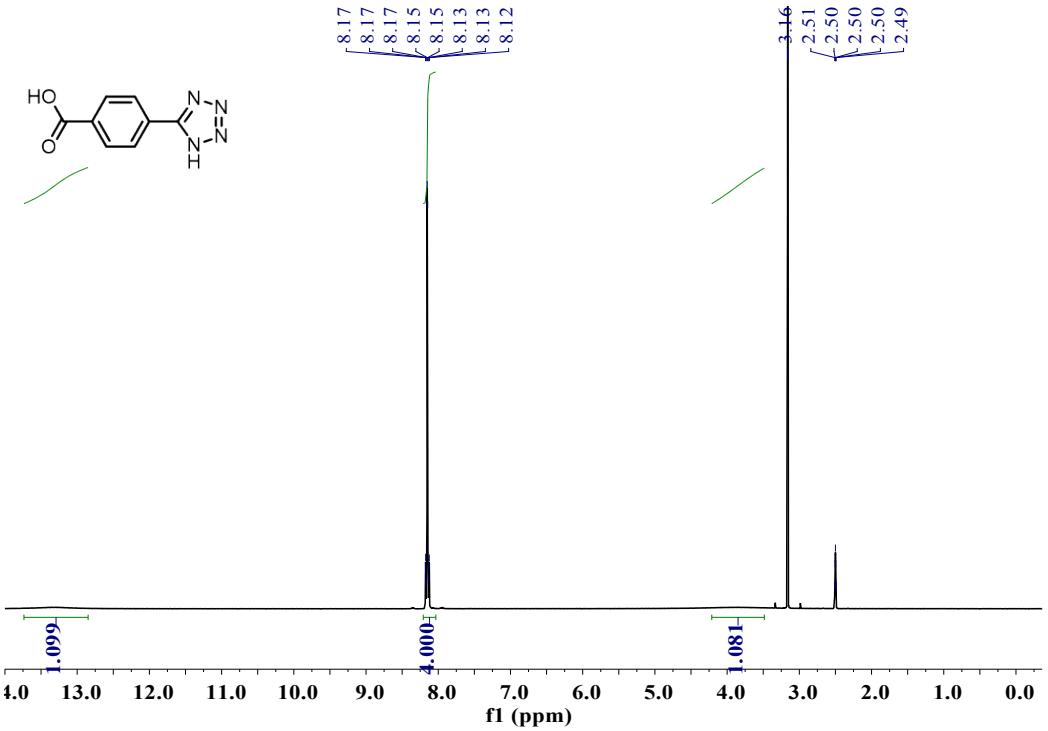

Figure S1. ^{1}H NMR spectrum of 4-tetrazole benzoic acid.

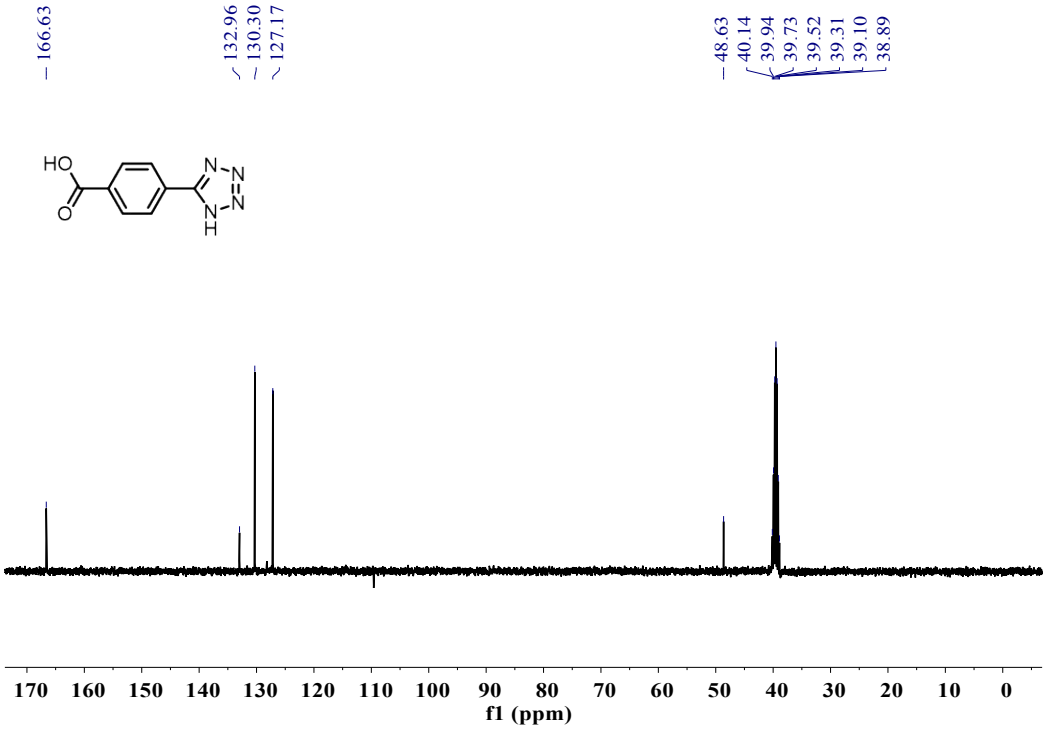

Figure S2. ^{13}C NMR spectrum of 4-tetrazole benzoic acid.

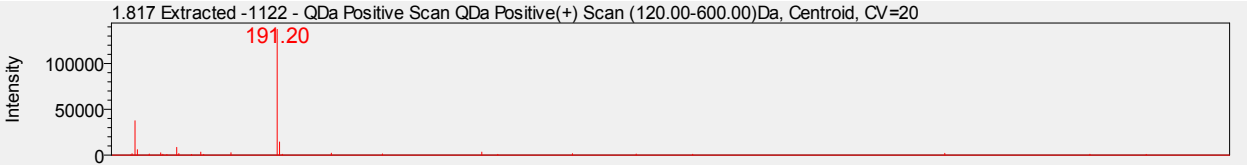

Figure S3. Mass spectrum of 4-tetrazole benzoic acid.

2.2 Preparation of CPF-5 crystal

CPF-5 was synthesized under solvothermal conditions according to a reported method with some modification [2,3]. Manganese chloride tetrahydrate (156 mg, 0.79 mmol), 4-tetrazole benzoic acid (4-TBA, 80 mg, 0.42 mmol) and ammonium formate (15 mg, 0.24 mmol) were dissolved in a mixture of DMF (2 mL) and water (0.2 mL) in a scintillation vial (24 mL). After sonication to make all solid dissolved homogeneously, the mixture was heated in an oven at 120 °C for 3 d. The resulted colorless crystals were separated by filtration while the mother liquid still warm to avoid the formation of amorphous precipitates. The crystals were washed with DMF (3 × 2 mL). The as-synthesized CPF-5 was immersed in acetonitrile (5 mL) at room temperature, after 12 h the solvent was decanted out. Then fresh acetonitrile was added and the above procedure was repeated for 3 times. The solid was activated under vacuum at 70 °C for 24 h.

2.4 Catalytic study

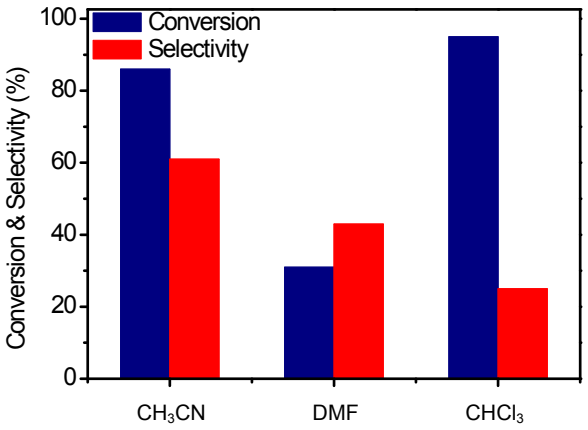

Figure S4. Oxidation of cyclohexene in different solvents. Reaction conditions: cyclohexene (0.2 mmol), CPF-5 (5 mg), *t*-BHP (2 equiv.), solvent (1 mL), 40 °C, 24 h. An O_2 balloon was attached to the reactor when used 0.1, 0.25, and 0.5 equiv. of *t*-BHP.

Table S1. Effect of radical inhibitor (BHT) on the cyclohexene oxidation over CPF-5.

Radical inhibitor	Conversion (%)	Selectivity (%)
-	19.3	57.1
BHT (3 equiv.)	Trace	-

Reaction conditions: cyclohexene (0.2 mmol), CPF-5 (5 mg), *t*-BHP (0.25 equiv.), BHT (0 or 3 equiv.), CH_3CN (1 mL), O_2 (1 bar), 40 °C, 4 h.

Table S2. Oxidation of cyclohexene catalyzed by different manganese catalysts.[a]

Entry	Catalyst	Conversion (%)	TON	Selectivity (%)[b]
1	CPF-5	16	1.5	53
2	$Mn(NO_3)_2$	3	0.3	41
3	$MnCO_3$	7	0.7	46
4	$Mn(OAc)_2$	6	0.6	45

[a] Reaction conditions: cyclohexene (0.2 mmol), catalyst (10.6 mol% of Mn), *t*-BHP (0.25 equiv.), CH_3CN (1 mL), O_2 (1 bar), 40 °C, 2 h. [b] Selectivity of 2-cyclohexene-1-one.

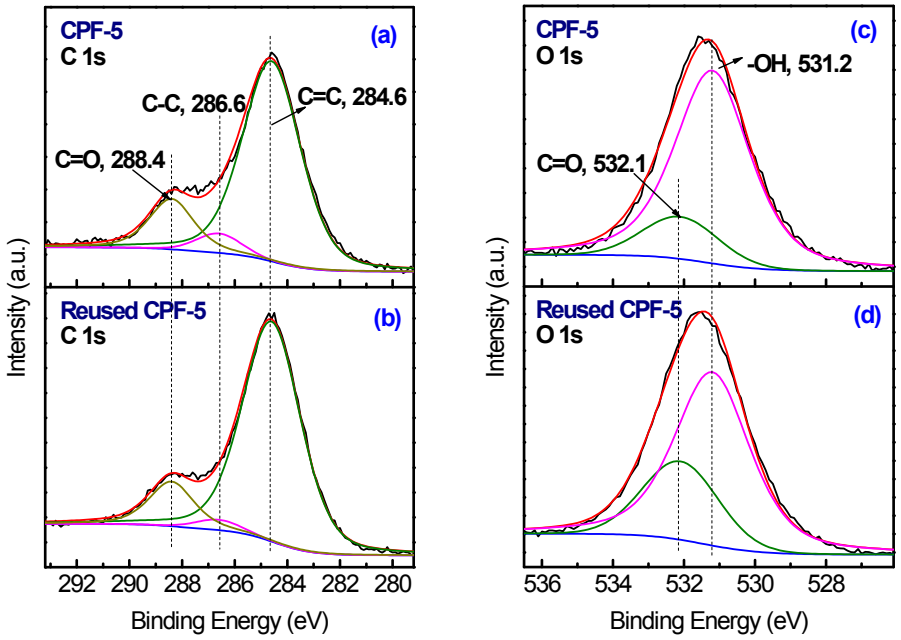

Figure S5. The XPS spectra of the fitted C 1s peak curves for (a) CPF-5 and (b) reused CPF-5; the fitted O 1s peak curves for (c) CPF-5 and (d) reused CPF-5.

Table S3. XPS peak position and percentage contributions of CPF-5 before and after catalysis.

		eV	%	
			CPF-5	Reused CPF-5
Mn $2p_{3/2}$	Mn^{IV}	642.5	33.3	41.4
	Mn^{III}	641.4	37.9	37.3
	Mn^{II}	640.4	28.7	21.2
C 1s	C=C	284.6	78.2	83.1
	C-C	286.6	5.3	2.8
	C=O	288.4	16.4	14.1
N 1s	N^+	400.9	19.4	20.8
	N-H, -N-N-	399.9	43.8	45.6
	=N-	399.0	36.8	33.6
O 1s	C=O	532.1	15.3	27.2
	-OH	531.2	84.7	72.8

Table S4. The relative ratio of elements on the surface of CPF-5 before and after catalysis.

Material	Area%			
	Mn	O	N	C
CPF-5	27.5	32.5	13.5	26.5
Reused CPF-5	26.2	33.8	13.1	26.9

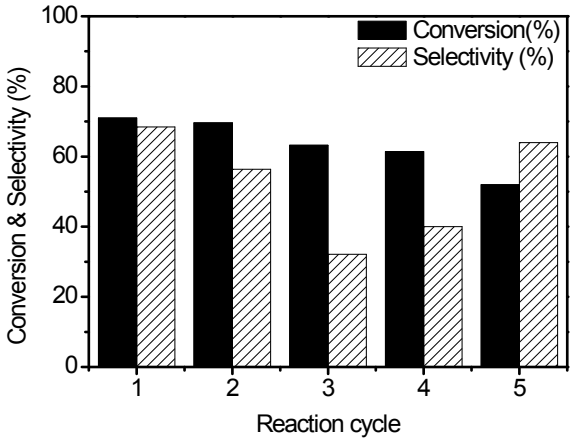

Figure S6. Recyclability test of CPF-5 in catalyzing the oxidation of cyclohexene. Reaction conditions: cyclohexene (0.2 mmol), CPF-5 (5 mg, 0.004 mmol based on Mn_5 SBU), *t*-BHP (70% solution in H_2O, 8.3 μL, 0.25 equiv.), CH_3CN (1 mL), 60 °C, O_2 (1 bar), 2 h.

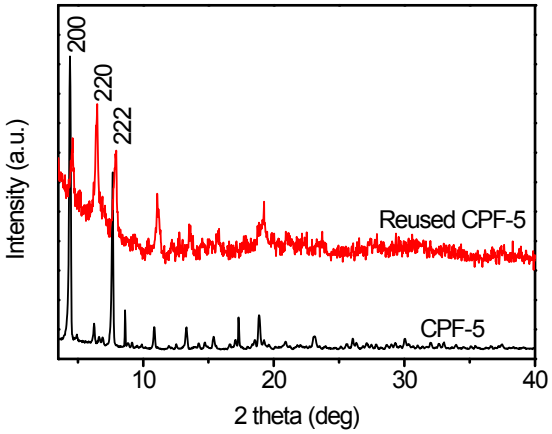

Figure S7. PXRD patterns of CPF-5 before and after catalytic oxidation reaction.

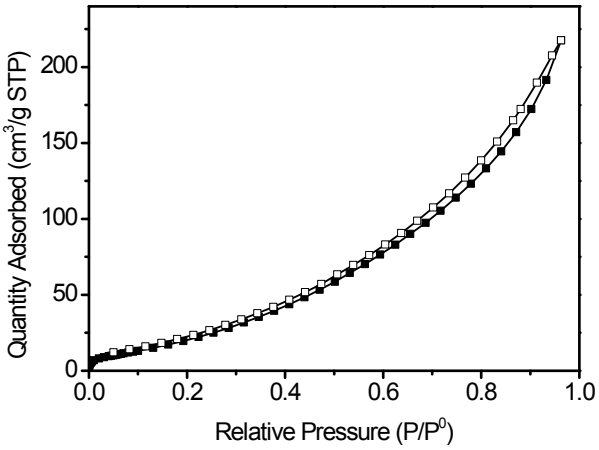

Figure S8. N_2-sorption isotherm of CPF-5 after five consecutive runs in the oxidation of cyclohexene. BET surface area: 164 $m^2 \cdot g^{-1}$.

Table S5. ICP-OES analysis result of CPF-5 before and after reaction.

Material	Mn content (wt%)
CPF-5	24
Reused CPF-5	27
Filtrate of the reaction[a]	0.006[b]

[a] Filtrate after a reaction time of 6 h. [b]The Mn content is referred to the total Mn amount in CPF-5.

Table S6. Selected MOFs and Manganese catalysts with catalytic activity toward oxidation of cyclohexene.

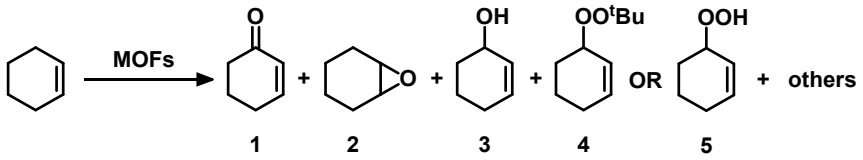

Catalyst	Oxidant	T(°C)	T(h)	Conv.(%)	Sel.(%)[ae]	Ref.
CPF-5	O_2 (1 bar)[a]	60	24	98	87	here
CPF-5	O_2 (1 bar)	60	24	95	62	here[af]
Fe_3O_4@Au/MOF-5	O_2 (13 bar)	80	8	45.5	80	4
$[Co^{II}Co_2^{III}(\mu_3\text{-O})(bdc)_3(tpt)]$[b]	*t*-BHP (1.0 equiv.)	70	24	63	14	5
	O_2 (1 bar)	70	24	38	20	5
Co(dpa)(2,2'-bipy)$(H_2O)_2$[c]	O_2 (1 MPa)	70	6	36.7	34.4	6
$\{[Cu_3Lu_2(ODA)_6(H_2O)_6]\cdot 10H_2O\}_n$[d]	*t*-BHP (1 equiv.)	75	24	60	57	7
	O_2 (5 bar)	120	4	95	60	7
$\{[CuMg(pdc)_2(H_2O)_4]\cdot 2H_2O\}_n$[e]	H_2O_2 (1.5 equiv.)	60	24	94	N.R.	8
ZrP⊂HKUST-1	O_2 (1 bar)	80	20	59.5	32.6	9
Co/Ni-MOF-74[f]	O_2 (1 bar)	80	N.R.	54.7	30	10
HKUST-1[g]	O_2 (1 bar)	80	5	45.7	44.9	11
$[Co(L\text{-}RR)(H_2O)\cdot H_2O]_\infty$[h]	*t*-BHP (0.5 equiv.)	70	24	18.6	N.R.	12
	O_2 (2 bar)	70	24	36.7	49	12
Fe-MIL-100	O_2 (1 bar)[i]	40	16	7	11	13
Cr-MIL-100	O_2 (1 bar)[i]	60	16	12	52	13
Fe-MIL-101	O_2 (1 bar)[j]	50	16	27	22	14,15
Cr-MIL-101	O_2 (1 bar)[j]	60	16	16	56	14,15
$[Cu_2(bipy)_2(btec)]_\infty$[k]	*t*-BHP (1 equiv.)	75	6	33	75	16
Cu^{2+}@COMOC-4[l]	O_2 +*i*-BA[l]	40	7	49	4.3	17
NH_2-MIL-47	O_2 +CHCA[m]	40	6	14.1	6[n]	18
NH_2-MIL-47 [Ti]	O_2 +CHCA[m]	40	6	25	12[n]	18
$[M_2(DOBDC)(H_2O)_2]\cdot 8H_2O$[o]	O_2 (1 bar)	80	20	34	17	19
$Cu_2(OH)(BTC)(H_2O)]n\cdot 2nH_2O$[p]	O_2 (1 bar)	80	20	22	7.5	19
NHPI/Fe(BTC)[q]	O_2 (1 bar)	100	2	9	47	20
	O_2 (5 bar)	100	5	12	59	20
Co-ZIF	O_2 +*i*-BA[r]	35	3	100	N.R.	21
NHPI+MFU-1	O_2 (1 bar)	35	24	35	5.6	22
MIL-101_D[t]	*t*-BHP (1.7 equiv.)	50	10	81	93	23
MIL-101_D[u]	*t*-BHP (1.7 equiv.)	50	10	92	88	23
[Cu(bpy)(H2O)2(BF4)2(bpy)[v]	O_2 (1 bar)	45	15	4.9[v]	89	24
$Mn_2^{(II,II)}(\mu_{1,1}\text{-4-}CH_3\text{-}C_6H_4COO)_2(phen)_4](ClO_4)_2$[w]	*t*-BHP (1.2 equiv.)	70	3	100	97.5	25
$Mn_2^{(II,II)}(\mu_{1,3}\text{-4-}CH_3\text{-}C_6H_4COO)_2(bipy)_4](ClO_4)_2$[x]	*t*-BHP (1.2 equiv.)	70	3	97	93.3	25

Cu(II)@UiO-66-NH_2	*t*-BHP (2 equiv.)	80	12	97	57	26
$[Mn(C_6H_5COO)(H_2O)(phen)_2](ClO_4)(CH_3OH)$[y]	*t*-BHP (7.4 equiv.)	70	6	94.3	76	27
$[Mn_2(\mu\text{-}C_6H_5COO)_2(bipy)_4]_2(ClO_4)$[z]	*t*-BHP (7.4 equiv.)	70	6	92.9	75.1	27
Cu-MOF-74	*t*-BHP	70	24	90	N.R.	28
Mn(II)/4'-Ar-2,2':6',2''-terpyridine complexes	*t*-BHP (2 equiv.)	50	6	58	47	29
Fe_3O_4@SiO_2@APTMS@VMIL-101	*t*-BHP (1.2 equiv.)	80	24	34	N.R.	30
Mn-analcime	*t*-BHP (1 equiv.)	35	24	68.2	46.4	31
MnTHPPOAc-MWCNT[aa]	*t*-BHP (2 equiv.)	r.t.	24	33	N.R.	32
Si/Al-APTMS-BPK-Mn	*t*-BHP (5 equiv.)	100	24	84	95	33
$Mn^{II}(Hsal\text{-}bhz)_2$/Y	*t*-BHP (1 equiv.)	75	14	94	93	34
$[Cu(H_2btec)(bipy)]$[ab]	*t*-BHP (1 equiv.)	75	24	61.8	11.9	35
[M(haacac)]-Al_2O_3[ac]	*t*-BHP (1.6 equiv.)	70	8	39.9	50.7	36
OMS-2[ad]	*t*-BHP (1 equiv.)	60	24	65	49	37

[a] 0.25 equiv. of *t*-BHP as additive. [b] bdc = benzene-1,4-dicarboxylate, tpt = 2,4,6-tri(4-pyridinyl)-1,3,5-triazine. 0.05 mmol, based on Co_3 SBU. [c] H_2dpa = 2,2'-diphenic acid, 2,2'-bipy = 2,2'-bipyridine. Molar ratio of Co/cyclohexene is 1:16000. [d] Ln^{III} = lanthanide ion, H_2ODA = 2,2'-oxydiacetic acid). [e] H_2Pdc = pyridine-2,5-dicarboxylic acid. [f] 60% of Co incorporated. [g] MOF crystal synthesized in CO_2-presented ionic liquid. [h] L-RR=(R,R)-thiazolidine-2,4-dicarboxylate. [i] Add 0.02-0.03 mmol of *t*-BHP as initiator. [j] With 0.02 mmol of *t*-BHP as additive. [k] H_4btec = 1,2,4,5-benzenetetracarboxylic acid. [l] COMOC=Center for Ordered Materials, Organometallics and Catalysis, Ghent University. [m] Cyclohexanecarboxaldehyde. [n] Yield of product. [o] Co-and Ni-MOF, DOBDC = 2,5-dihydroxyterephthalic acid. [p] BTC = 1,3,5-benzenetricarboxylic acid. [q] NHPI = *N*-hydroxyphthalimide. [r] Isobutyraldehyde (32 mmol), O_2 (7–10 ml/min). [s] Atmospheric oxygen, NHPI (50 mg, 0.31 mmol), MFU-1 (15 mg, 0.038 mmol based on cobalt centres), 1,2,4-trichlorobenzene (150 μL, 1.2 mmol; internal standard), educt (3.0 mmol; cyclohexene (300 μL). [t] Activated at 180 °C. [u] MIL-101 was prepared with enlarged surface area and activated in vacuum at 180 °C. [v] bpy: 4,4'-bipyridine. Conversion is calculated from the amount of product formed. [w] phen = 1,10-phenanthroline. [x] phen = bipy = 2,2-bipyridine. [y] phen = 1,10-phenanthroline. [z] bipy =2,2'-bipyridine. [aa] Carbon nanotube supported iron(III) and manganese(III) complexes ofmeso-tetrakis(4-hydroxyphenyl)porphyrin. [ab] H_4btec = 1,2,4,5-benzenetetracarboxylic acid. [ac] H_2haacac = bis(2-hydroxyanil)acetylacetone. [ad] Manganese oxide octahedral molecular sieves with a cryptomelane structure. [ae] Selectivity of 2-cyclohexen-1-one. N.R.: not reported. [af] Cyclohexene (1 mL), CPF-5 (20 mg, 0.25 mol% of Mn), solvent free, 60 °C, 24 h, O_2 (1 bar).

References

1. P. Pachfule, Y. Chen, S. C. Sahoo, J. Jiang and R. Banerjee, *Chem. Mater.*, 2011, **23**, 2908-2916.
2. L. Wang, C. E. Moore and S. M. Cohen, *Cryst. Growth Des.*, 2017, **17**, 6174-6177.
3. L. Wang, J. Morales, T. Wu, X. Zhao, W. P. Beyermann, X. H. Bu and P. Y. Feng, *Chem. Commun.*, 2012, **48**, 7498-7500.
4. M. Kohantorabi and M. R. Gholami, *Mater. Chem. Phys.*, 2018, **213**, 472-481.
5. T. Zhang, Y.-Q. Hu, T. Han, Y.-Q. Zhai and Y.-Z. Zheng, *ACS Appl. Mater. Interfaces*, 2018, **10**, 15786-15792.
6. X. Feng, J. Hao, Y. Gao, W. Bai, Y. Cheng, F. Wang, L. Han, Q. Suo and Y. Wang, *Catal. Commun.*, 2018, **104**, 48-52.
7. P. Cancino, V. Paredes-García, J. Torres, S. Martínez, C. Kremer and E. Spodine, *Catal. Sci. Technol.*, 2017, **7**, 4929-4933.
8. D. Saha, D. K. Hazra, T. Maity and S. Koner, *Inorg. Chem.*, 2016, **55**, 5729-5731.
9. Y. Kan and A. Clearfield, *Inorg. Chem.*, 2016, **55**, 5634-5639.
10. D. Sun, F. Sun, X. Deng and Z. Li, *Inorg. Chem.*, 2015, **54**, 8639-8643.
11. C. Liu, B. Zhang, J. Zhang, L. Peng, X. Kang, B. Han, T. Wu, X. Sang and X. Ma, *Chem. Commun.*, 2015, **51**, 11445-11448.
12. G. Tuci, G. Giambastiani, S. Kwon, P. C. Stair, R. Q. Snurr and A. Rossin, *ACS Catal.*, 2014, **4**, 1032-1039.
13. O. A. Kholdeeva, I. Y. Skobelev, I. D. Ivanchikova, K. A. Kovalenko, V. P. Fedin and A. B. Sorokin, *Catal. Today*, 2014, **238**, 54-61.
14. Skobelev, I. Y. Skobelev, K. A. Kovalenko, V. P. Fedin, A. B. Sorokin and O. A. Kholdeeva, *Kinet. Catal.*, 2013, **54**, 607-614.
15. I. Y. Skobelev, A. B. Sorokin, K. A. Kovalenko, V. P. Fedin and O. A. Kholdeeva, *J. Catal.*, 2013, **298**, 61-69.
16. P. Cancino, V. Paredes-García, P. Aguirre and E. Spodine, *Catal. Sci. Technol.*, 2014, **4**, 2599-2607.
17. Y.-Y. Liu, K. Leus, T. Bogaerts, K. Hemelsoet, E. Bruneel, V. Van Speybroeck and P. Van Der Voort, *ChemCatChem*, 2013, **5**, 3657-3664.
18. K. Leus, G. Vanhaelewyn, T. Bogaerts, Y.-Y. Liu, D. Esquivel, F. Callens, G. B. Marin, V. Van Speybroeck, H. Vrielinck and P. Van Der Voort, *Catal. Today*, 2013, **208**, 97-105.
19. Y. Fu, D. Sun, M. Qin, R. Huang and Z. Li, *RSC Adv.*, 2012, **2**, 3309-3314.
20. A. Dhakshinamoorthy, M. Alvaro and H. Garcia, *J. Catal.*, 2012, **289**, 259-265.
21. A. Zhang, L. Li, J. Li, Y. Zhang and S. Gao, *Catal. Commun.*, 2011, **12**, 1183-1187.
22. M. Tonigold, Y. Lu, A. Mavrandonakis, A. Puls, R. Staudt, J. Möllmer, J. Sauer and D. Volkmer, *Chem.—Eur. J.*, 2011, **17**, 8671-8695.
23. N. V. Maksimchuk, K. A. Kovalenko, V. P. Fedin and O. A. Kholdeeva, *Adv. Synth. Catal.*,

2010, **352**, 2943-2948.
24. D. Jiang, T. Mallat, D. M. Meier, A. Urakawa and A. Baiker, *J. Catal.*, 2010, **270**, 26-33.
25. Y. Kılıç and İ. Kani, *Polyhedron*, 2018, **141**, 352-359.
26. J.-C. Wang, Y.-H. Hu, G.-J. Chen and Y.-B. Dong, *Chem. Commun.*, 2016, **52**, 13116-13119.
27. I. Kani and S. Bolat, *Appl. Organometal. Chem.*, 2016, **30**, 713-721.
28. D. Ruano, M. D í az-García, A. Alfayate and M. Sánchez-Sánchez, *ChemCatChem*, 2015, **7**, 674-681.
29. B. Liu, W. Luo, H. Li, X. Qi and Q. Hu, *Synth. React. Inorg. Me.*, 2015, **45**, 1097-1101.
30. F. Farzaneh and Y. Sadeghi, *J. Mol. Catal. A: Chem.*, 2015, **398**, 275-281.
31. A. Bejar, S. Ben Chaabene, M. Jaber, J.-F. Lambert and L. Bergaoui, *Microporous Mesoporous Mater.*, 2014, **196**, 158-164.
32. S. Rayati, P. Jafarzadeh and S. Zakavi, *Inorg. Chem. Commun.*, 2013, **29**, 40-44.
33. D. Habibi and A. R. Faraji, *Appl. Surf. Sci.*, 2013, **276**, 487-496.
34. M. Bagherzadeh and M. Zare, *J. Coord. Chem.*, 2012, **65**, 4054-4066.
35. P. Aguirre, K. Brown, D. Venegas-Yazigi, V. Paredes-García and E. Spodine, *Macromol. Symp.*, 2011, **304**, 65-71.
36. M. Salavati-Niasari and S. H. Banitaba, *J. Mol. Catal. A: Chem.*, 2003, **201**, 43-54.
37. R. Ghosh, Y.-C. Son, V. D. Makwana and S. L. Suib, *J. Catal.*, 2004, **224**, 288-296.